NACA RM L50H10

NACA

RESEARCH MEMORANDUM

INITIAL FLIGHT INVESTIGATION OF A TWIN-ENGINE SUPERSONIC RAM JET

By Maxime A. Faget and H. Rudolph Dettwyler

Langley Aeronautical Laboratory
Langley Air Force Base, Va.

NATIONAL ADVISORY COMMITTEE
FOR AERONAUTICS

WASHINGTON

September 15, 1950

NATIONAL ADVISORY COMMITTEE FOR AERONAUTICS

RESEARCH MEMORANDUM

INITIAL FLIGHT INVESTIGATION OF A TWIN-ENGINE SUPERSONIC RAM JET

By Maxime A. Faget and H. Rudolph Dettwyler

SUMMARY

A flight investigation was made of a supersonic twin-ram-jet test vehicle using short-flame-length burners. The test demonstrated a maximum acceleration of 3.6g and a maximum flight Mach number of 3.02. Data were obtained over a Mach number range from about 1.9 to 3.0, an altitude range from 1,800 to 40,900 feet, and a fuel-air-ratio range from 0.012 to 0.065. Over these ranges an over-all combustion efficiency of 81 percent and an over-all fuel specific impulse of 1,059 seconds were demonstrated.

INTRODUCTION

A ducted-tail ram jet was proposed in reference 1 as having compactness, a large useful volume, and easily accessible controls. The theoretical analysis presented in this reference indicated the possibility of high performance for such configurations and the necessity of developing short-flame-length burners in order that these advantages be realized. A short-flame-length burner employing a combustion chamber of only 19.7 inches was developed jointly by the Lewis and Langley Laboratories of the National Advisory Committee for Aeronautics. Initial development of the short-flame-length burner is reported in reference 2. In its present form the burner is regenerative with fuel-cooled flame holders necessitated by the very high specific-heat release in the combustion chamber of over 2.5×10^6 British Thermal Units per minute per cubic foot.

A method of rapidly igniting this burner in flight during the period that the ram jet is being boosted up to operating velocity has been developed by ground tests. The performance of the first ground-launched test vehicle employing the short-flame-length burner in twin ram jets installed on the vehicle tail surfaces with ignition during flight is presented in this paper.

APPARATUS AND TEST

Test Vehicle

A plan view and a side-elevation view of the test vehicle with twin ram jets installed on the tail surfaces is shown in figure 1(a). In the plan view in figure 1(a) and in the close-up view in figure 1(b), the combustor shell has been removed from one ram jet to show the short-flame-length burner. The assembled test vehicle together with the double-rocket-booster unit used for launching is shown in figure 2.

The principal dimensions and general arrangement of the test vehicle are shown in figure 3. The vehicle was 15 feet $9\frac{1}{2}$ inches long and weighed 246 pounds, including 25 pounds of fuel. The twin ram jets were 6.6 inches in outside diameter, were 50.2 inches long, and were mounted symmetrically on the horizontal fin at a distance of 8.55 inches from the vehicle center line. The 8-inch-diameter fuselage of the vehicle was compartmented from front to rear as follows: telemeter nose antenna, telemeter section, telemeter and fuel-control power-supply section, fuel tank, fuel-control section, telemeter pressure cell section, and booster-unit adapter. The cone-cylinder fuselage with a fineness ratio of 23.7 was selected as a simple low-drag configuration.

Ram-Jet Engines

Two identical ram jets mounted on the horizontal tail surfaces were used to power the vehicle. Each engine was 6.6 inches in diameter, 50.2 inches long, and weighed 35.6 pounds. Figure 4 is a sectional view of the engine showing component parts. An inlet diffuser of the Ferri type, similar to those described in reference 3, employing a 40° cone was used with a design Mach number of 2.13 and a diffuser area ratio of 2.69. The contraction ratio of the exit nozzle was 0.783. These area ratios were selected to cover a speed range from $M = 1.8$ to $M = 3.0$.

A burner was used having three doughnut-shaped flame holders mounted in line with and directly behind a fuel-spray ring of the same size and shape. This burner is designated the "donut" burner and is illustrated in figure 5. The flame holders and fuel-spray ring were constructed as a unit and were mounted on the main fuel feed tube. The fuel passed through and cooled both the flame holders and supporting structure before entering the spray ring.

Fuel was sprayed through 50 No. 43 drill-size holes. These holes were arranged as follows: 24 equally spaced on the outer rim of the spray ring, 18 equally spaced on the inner rim of the spray ring, and 8 holes, 2 on each fuel-supply tube directly behind the spray ring. The flame holders and spray ring were stamped from $\frac{1}{32}$-inch Inconel sheet and welded. The fuel-feed tubes were $\frac{1}{32}$-inch wall Inconel tubing.

This type of burner permits the use of a very short combustion chamber, in this case 19.7 inches from the fuel-spray ring to the exit nozzle. The combustion-chamber shell was constructed from 0.05-inch Inconel sheet, with an inside diameter of 6.50 inches and a length of 21.1 inches. The exit nozzle was made of 1020 steel.

Since the booster accelerated the vehicle to operating speed in only 3 seconds, a simple, reliable, fast-acting starting technique was developed in a series of ground tests. The engines were ignited by two electric delay squibs in each combustion chamber. These squibs fired 2.45 seconds after take-off when the vehicle was at $M = 1.50$. In order to permit ignition, a $\frac{3}{32}$-inch-thick magnesium starting disk blocking 69 percent of the area was attached to the last flame holder (as illustrated in fig. 5). These disks restricted the velocity at the combustion-chamber entrance and allowed proper mixing of fuel and air prior to ignition. Approximately 0.7 second after ignition the disks were burned away and the engines operated normally. The ground-test investigation indicated that a reduced fuel-air ratio was required to insure dependable starts. Therefore, the fuel-metering valve was constructed so that the fuel rate from 2 to 3.5 seconds was 0.40 pound per second; a mean fuel-air ratio of 0.027 was thereby obtained.

Fuel Supply and Regulation

The fuel used was ethylene (C_2H_4). This fuel was carried as a vapor in a 1.37-cubic-foot high-pressure tank at 1,200 pounds per square inch gage. The fuel rate was controlled by a special motorized needle valve. The needle of this valve was extra long and cut to a particular taper in such a way that the fuel was metered at a predetermined rate for 12 seconds. After the first 12 seconds, fuel flow continued at a decreased rate. In addition to metering the fuel this valve was equipped with a switch for firing the boosters as well as firing electric delay squibs that ignited the ram-jet engines during flight. In this way the fuel metering was synchronized with the time of take-off and the time of engine ignition during flight. The use of highly pressurized vapor fuel presented some advantages. There was no sloshing of fuel in the tank, and a positive supply of fuel was maintained during both positive

and negative acceleration. Also, the fuel supplied its own metering and injection pressure without the use of pumps.

Booster

A sketch of the booster assembly is presented in figure 6. Two 6.25-inch ABL Deacon rocket motors (3.5 ES-5700), each with a total impulse of 20,000 pound-seconds, were mounted side by side and fired simultaneously. The rocket head caps were mounted in a magnesium casting which also served as the female end of the coupling to the test vehicle. The rear ends of the rockets were joined by the fin structure. The booster carried four fins, each with an area of 2.5 square feet.

Instrumentation

Continuous-wave Doppler radar near the launching site was used to measure velocity of the test vehicle for the first 12.5 seconds of the flight. The flight path of the vehicle was obtained by NACA modified SCR-584 tracking radar during the first 38 seconds of flight.

An NACA six-channel telemeter measured total pressure, longitudinal acceleration, and static pressures at the points shown in figure 4. In addition, the total-pressure channel was pulsed by a revolution counter on the metering valve to indicate valve position. All telemeter channels recorded data throughout the flight to impact (136 seconds after take-off).

Immediately after flight a balloon carrying a radiosonde was released to obtain atmospheric conditions.

Flight Test

Flight test of the model was conducted at the Pilotless Aircraft Research Station at Wallops Island, Va. Since the model followed a zero-lift trajectory, it was launched at 45° in order that a range of altitudes would be traversed. Fuel flow was started 1.5 seconds after take-off. Ignition of ram jets occurred at 2.45 seconds after take-off at $M = 1.50$. Three seconds after take-off the booster separated after accelerating the vehicle to $M = 1.89$, and during the next 15.5 seconds the test vehicle accelerated to a velocity of 3,019 feet per second. A peak Mach number of 3.02 was attained at a velocity of 2,979 feet per second 3 seconds later. A maximum acceleration of 3.6g was recorded during this time. Combustion was sustained to an altitude of 40,900 feet. Burnout occurred at a fuel-air ratio of 0.012 at 28.96 seconds and 29.52 seconds for the left and right engines, respectively. The vehicle

coasted to a peak altitude of 56,340 feet and to a horizontal range of 36.1 miles at impact. A trajectory of the flight is presented in figure 7.

ANALYSIS OF DATA AND DISCUSSION

The accelerometer data were used to determine the flight path and the velocity-time history of the vehicle beyond the ranges of the tracking radars. The total-pressure data, together with atmospheric data obtained from the radiosonde, were used to determine the velocity independently. Figure 8 shows a Mach number time curve of the flight determined by three methods: Doppler radar extended by integration of accelerometer data, differentiation of SCR-584 radar data, and total-pressure and atmospheric-pressure data. Good agreement is shown between these three methods; however, the Mach number determined by the Doppler radar and accelerometer is considered to be most accurate and was used in the computation of performance. Included in figure 8 is a time history of the longitudinal acceleration. Figure 9 presents the atmospheric temperature and pressure encountered by the model plotted against flight time.

Figure 10 shows a time history of the static pressures measured in the engines. This curve shows the time of ignition at 2.45 seconds and the time required for the starting disk to burn out. The starting disk was placed between the two static-pressure orifices. Therefore, as the starting disk burned away, diffuser exit pressure dropped and combustion-chamber exit pressure rose. The pressure records indicate that the starting disks were completely burned away by 3.5 seconds. The drop in static pressure at approximately 12 seconds was due to a drop in engine thrust, whereas a final drop at 29 seconds indicated the time of engine burnout.

An indication that both engines operated at nearly equal thrust is shown by the close agreement between the measured engine static pressures. All engine pressures as well as the accelerometer produced smooth traces on the telemeter record, indicating that the ram jets operated smoothly.

The diffuser recovery calculated from the diffuser-exit static pressure (fig. 10) is shown in figure 11. The low diffuser recovery indicates that the ram jets were not operating at maximum thrust conditions. Reference 3 indicates that much higher diffuser recoveries are possible. Greater diffuser recovery would have been encountered if the fuel-air ratio had been greater or if the combustion-chamber exit nozzles had smaller throats. The diffuser recovery was essentially determined before launching by the area ratio chosen and the fuel rate selected. Ground-test experience showed violent diffuser buzz, with a

resulting decrease in thrust, at fuel-air ratios greater than that required for maximum diffuser recovery. Since adequate thrust could be obtained at a lower diffuser recovery, optimum recovery was not sought in this test in order to avoid the possibility of diffuser buzz.

The net thrust was determined from the absolute acceleration (fig. 8) and the vehicle mass, corrected for fuel consumption. Net thrust coefficient was then determined using the atmospheric conditions shown in figure 9. In a similar manner the total drag coefficient after burnout was determined over a range of Mach numbers from 3.0 to 1.80. The internal drag coefficient was then calculated from the engine geometry by use of the equations of continuity and momentum. The external drag coefficient was determined by subtracting the calculated internal drag coefficient from the measured total drag coefficient. The external drag coefficient at the various Mach numbers was then added to the net thrust coefficient to give gross thrust coefficient. Figure 12 shows the measured total drag coefficient, the internal drag coefficient, and the resulting external drag coefficient based on fuselage frontal area. The external drag coefficient was higher than was expected. It is likely that some unfavorable interference effects between the body and nacelles may have been encountered. Figure 13 presents the net thrust coefficient and gross thrust coefficient plotted against flight Mach number.

The over-all engine performance was evaluated by determining the total engine impulse and the total fuel required, complete heat release being assumed. These values were compared with actual fuel consumption to determine over-all fuel specific impulse and over-all combustion efficiency. The gross thrust coefficient based on combustion-chamber cross-section areas was calculated from the gross thrust coefficient curve based on body area. From the various values of gross thrust coefficient, Mach number, and free-stream temperatures throughout the burning portion of flight, fuel-air ratios were calculated, complete heat release being assumed. Figure 14 shows the gross thrust coefficient based on combustion-chamber areas and the calculated fuel-air ratio against flight Mach number. A maximum thrust coefficient of 0.72 at Mach number 2.175 is shown. The thrust-coefficient dip at $M = 2.7$ was due to the fuel rate decreasing after the metering needle in the valve was completely withdrawn. The curves reversed after $M = 3.02$ because the flight speed decreased while the engines were still operating at decreased thrust.

The fuel rate was determined before flight by several blowdowns of the tank using the same quantity of fuel and the same metering valve. Since the valve ran at the same speed both during flight and ground tests, the ground-test fuel rate should approximate the fuel rate during flight, except for the effect of aerodynamic heating. The ground-test fuel rate, although not considered to be accurate for flight conditions,

indicated that a maximum fuel-air ratio of approximately 0.065 was encountered at about $M = 2.68$ and that the minimum fuel-air ratio of 0.012 was encountered at burnout. The gross thrust, fuel rate determined from ground test, and calculated fuel rates are plotted against time in figure 15. Integration of the thrust-time curve from 3.5 to 29.5 seconds gives a total impulse of 25,204 pound-seconds during this interval. Integration of the ground-test fuel rate over the same interval showed a total fuel consumption of 23.8 pounds; this fuel consumption is believed to be the quantity of fuel used by the engines during this interval. Integration of the calculated fuel rates during the same interval indicated that 19.23 pounds of fuel would be required if complete heat release were obtained. By dividing the total impulse by the fuel consumed by the engines, an over-all specific impulse of 1,059 seconds was obtained. Similarly, the ratio of fuel consumption calculated for complete heat release to fuel consumed by the engines gave an over-all combustion efficiency of 81 percent. These values were obtained for the complete burning portion of the flight and under conditions ranging from 1,800 to 40,900 feet altitude, Mach numbers from 1.89 to 3.02, and fuel-air ratios from 0.012 to 0.065.

SUMMARY OF RESULTS

In this free-flight investigation of a ram-jet test vehicle the following points were observed:

1. Both ram-jet engines operated satisfactorily over the following range of conditions: the fuel-air-ratio range of 0.012 to 0.065, an altitude range from 1,800 to 40,900 feet, and a Mach number range from 1.89 to 3.02.

2. Successful engine ignition was accomplished by electric delay squibs and a starting disk at a fuel-air ratio of 0.027 and $M = 1.50$ at 1,800 feet altitude.

3. An over-all combustion efficiency of 81 percent and a fuel specific impulse of 1,059 seconds were indicated from the flight results.

4. The maximum thrust coefficient of 0.72 was obtained at $M = 2.175$.

5. A maximum longitudinal acceleration of 3.6g was recorded.

Langley Aeronautical Laboratory
National Advisory Committee for Aeronautics
Langley Air Force Base, Va.

REFERENCES

1. Hill, Paul R., and Gammal, A. A.: An Analysis of Ducted-Airfoil Ram Jets for Supersonic Aircraft. NACA RM L7I24, 1948.

2. Breitwieser, Roland: Performance of a Ram-Jet-Type Combustor with Flame Holders Immersed in the Combustion Zone. NACA RM E8F21, 1948.

3. Ferri, Antonio, and Nucci, Louis M.: Preliminary Investigation of a New Type of Supersonic Inlet. NACA RM L6J31, 1946.

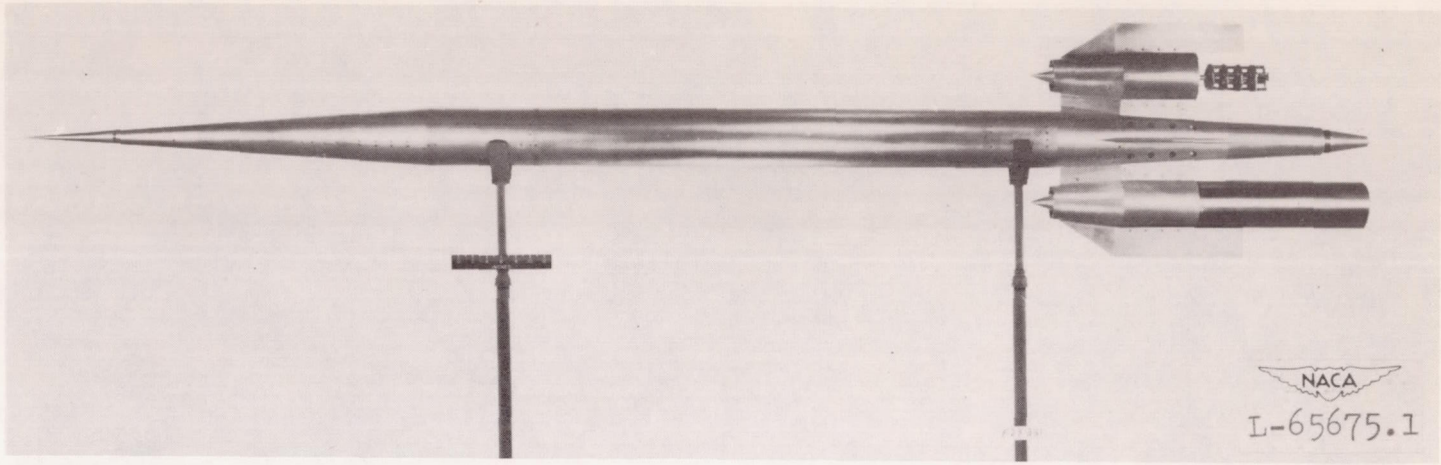

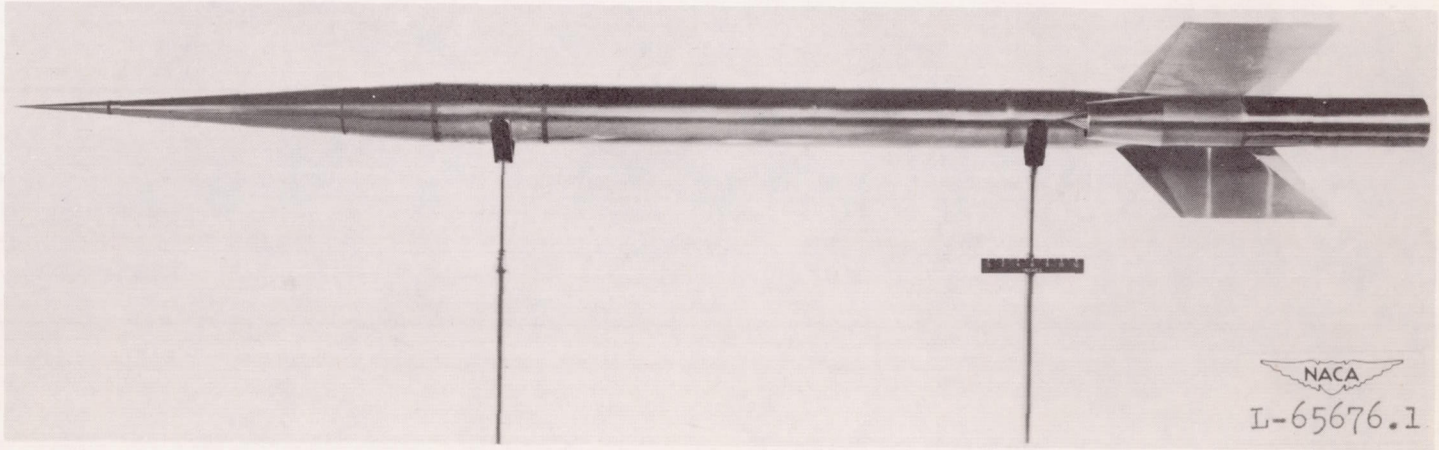

(a) Over-all view of test vehicles.

Figure 1.- Ram-jet test vehicle.

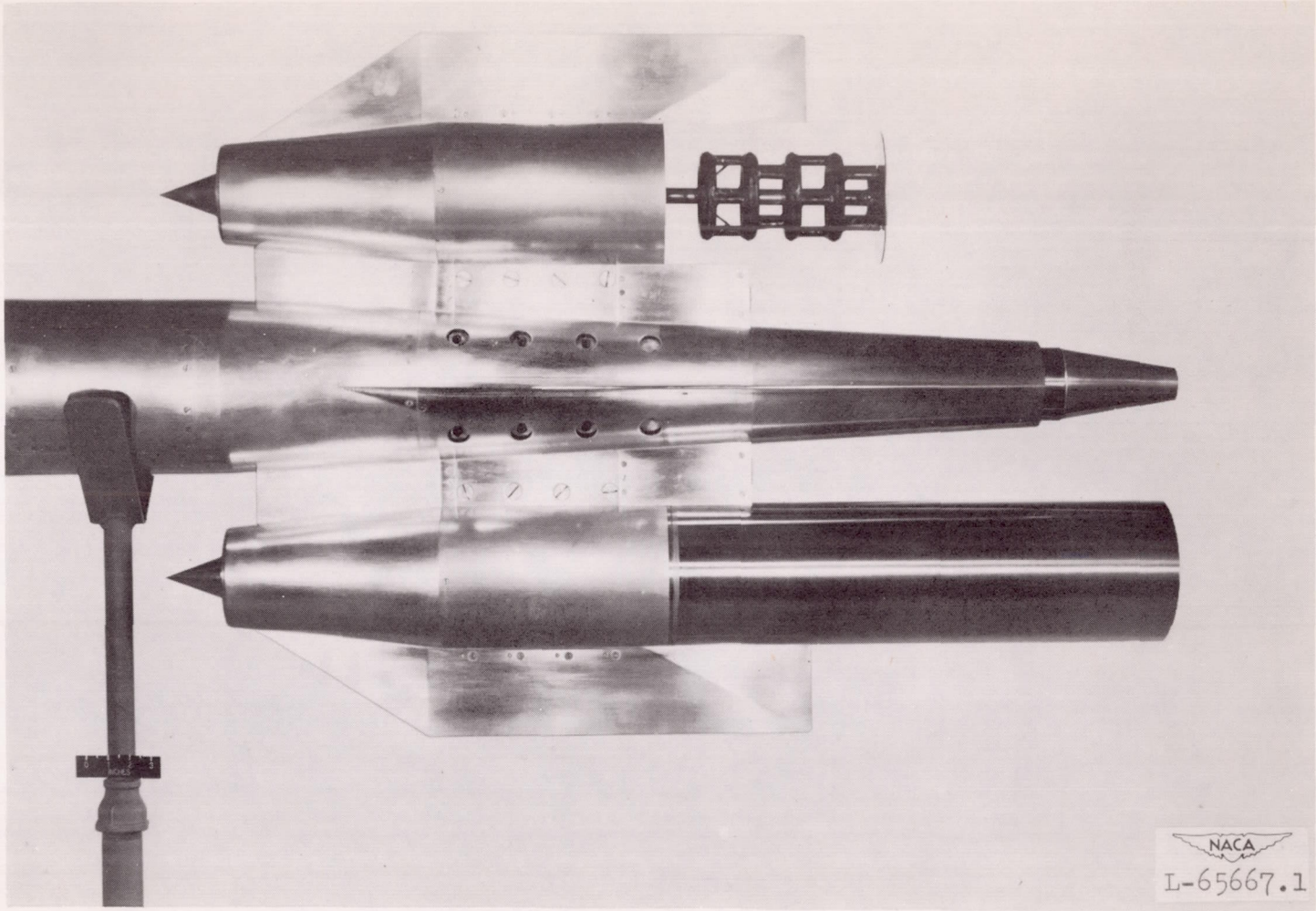

(b) Close-up view of ram-jet engines with and without combustor shell.

Figure 1.- Concluded.

Figure 2.- Test vehicle and booster on launcher.

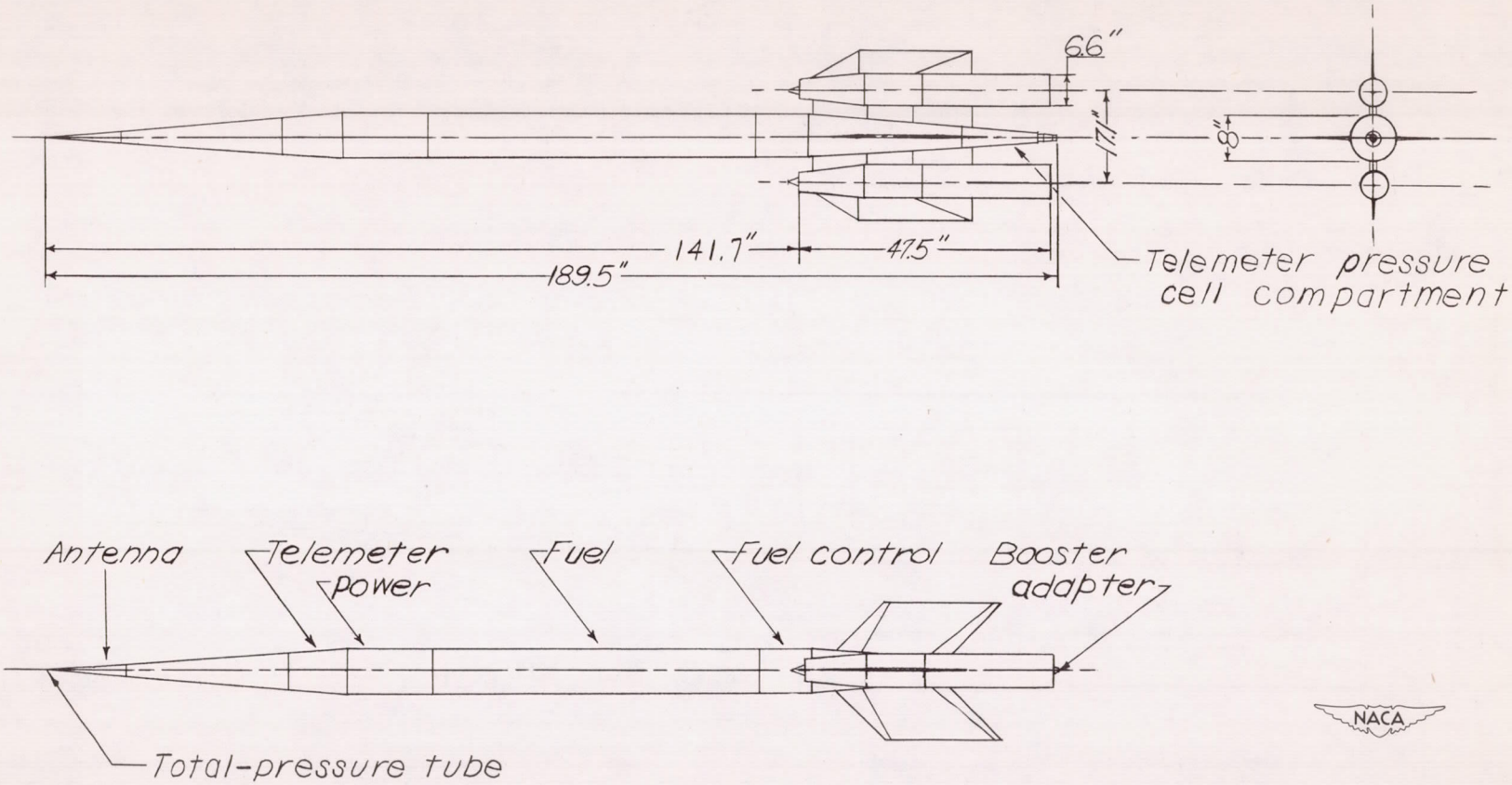

Figure 3.- General arrangement of test vehicle.

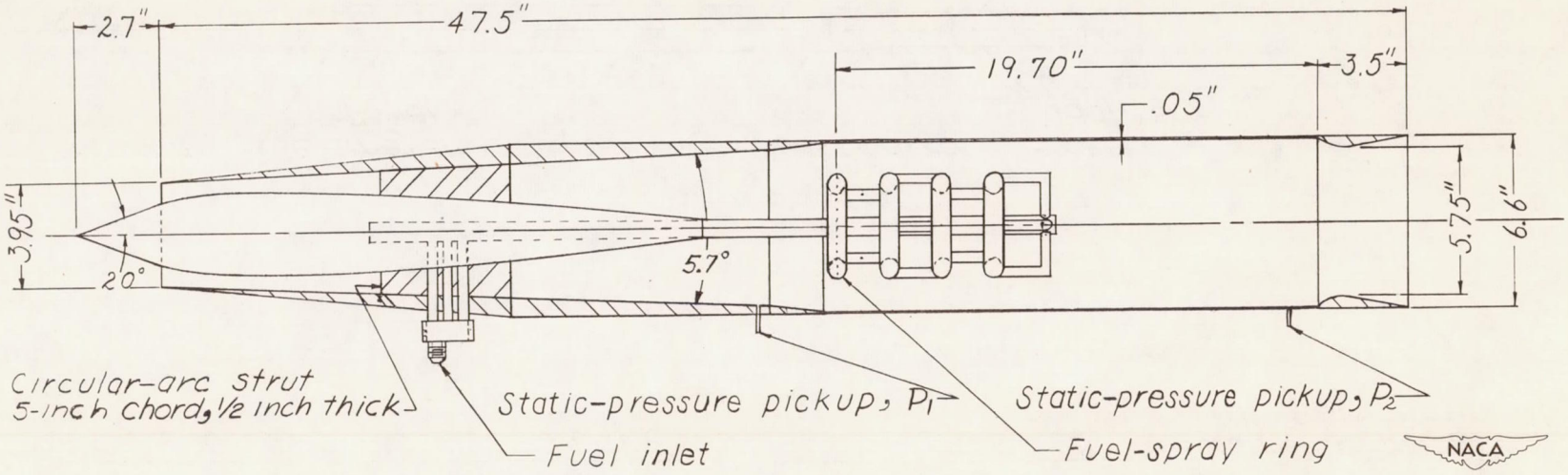

Figure 4.- Nacelle-type ram-jet engine tested.

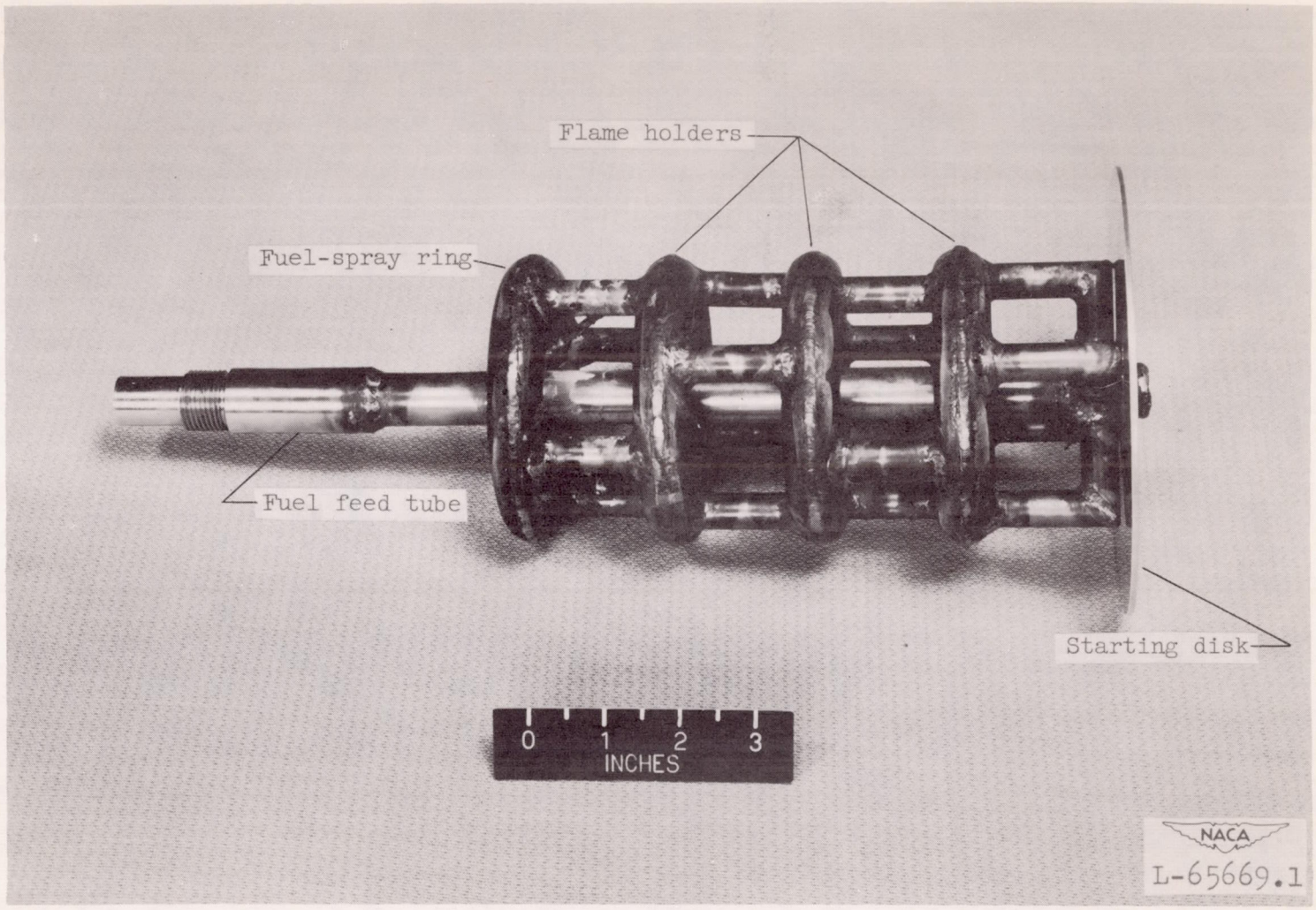

Figure 5.- Three-row donut burner with starting disk.

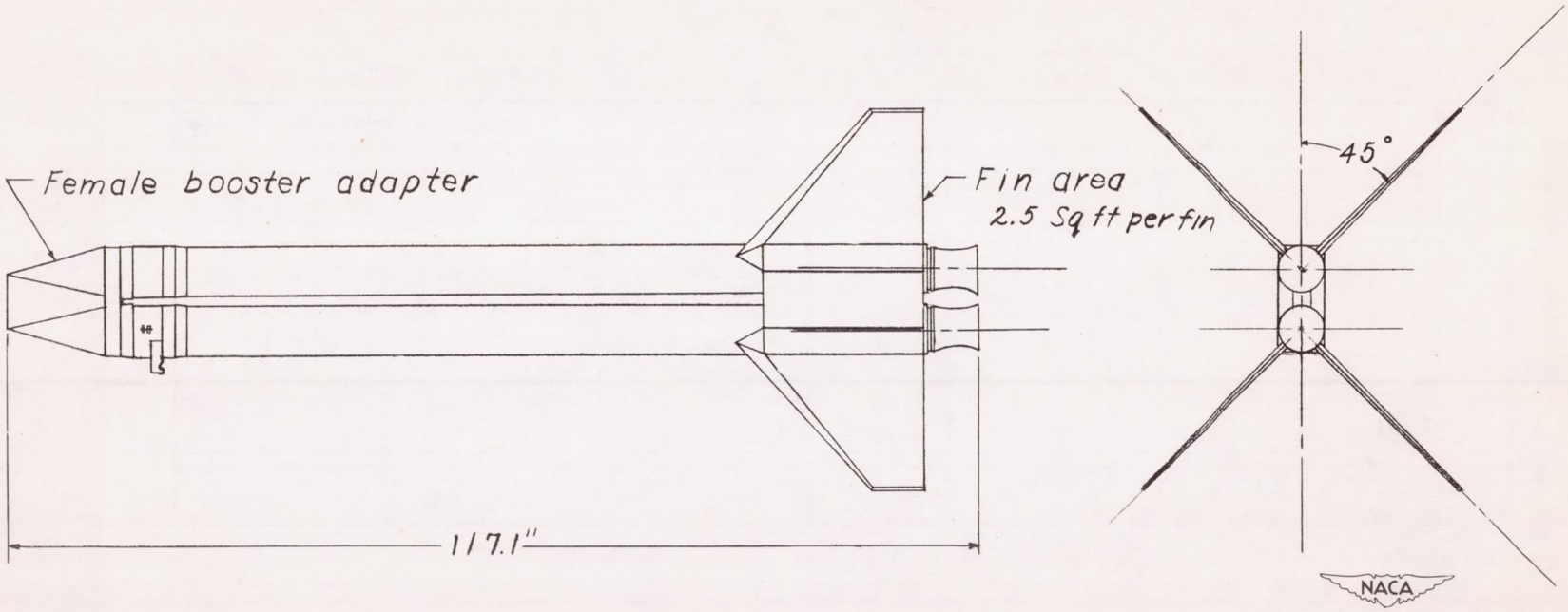

Figure 6.- Double Deacon booster.

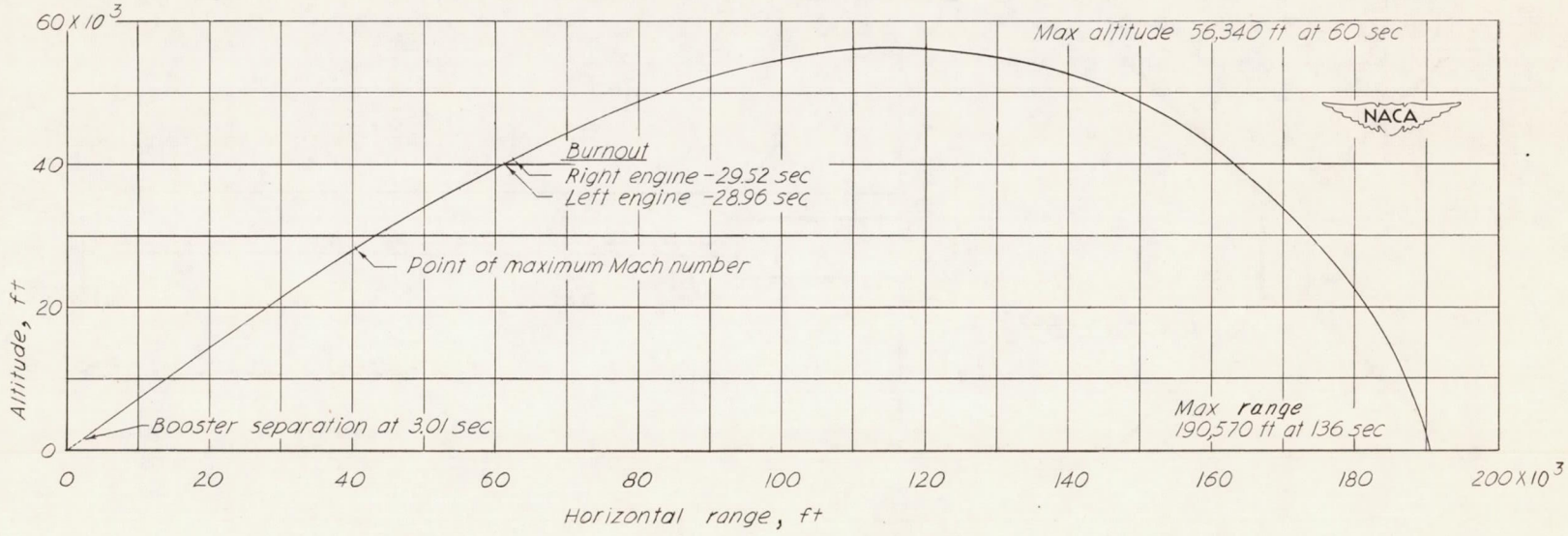

Figure 7.- Flight trajectory of test vehicle.

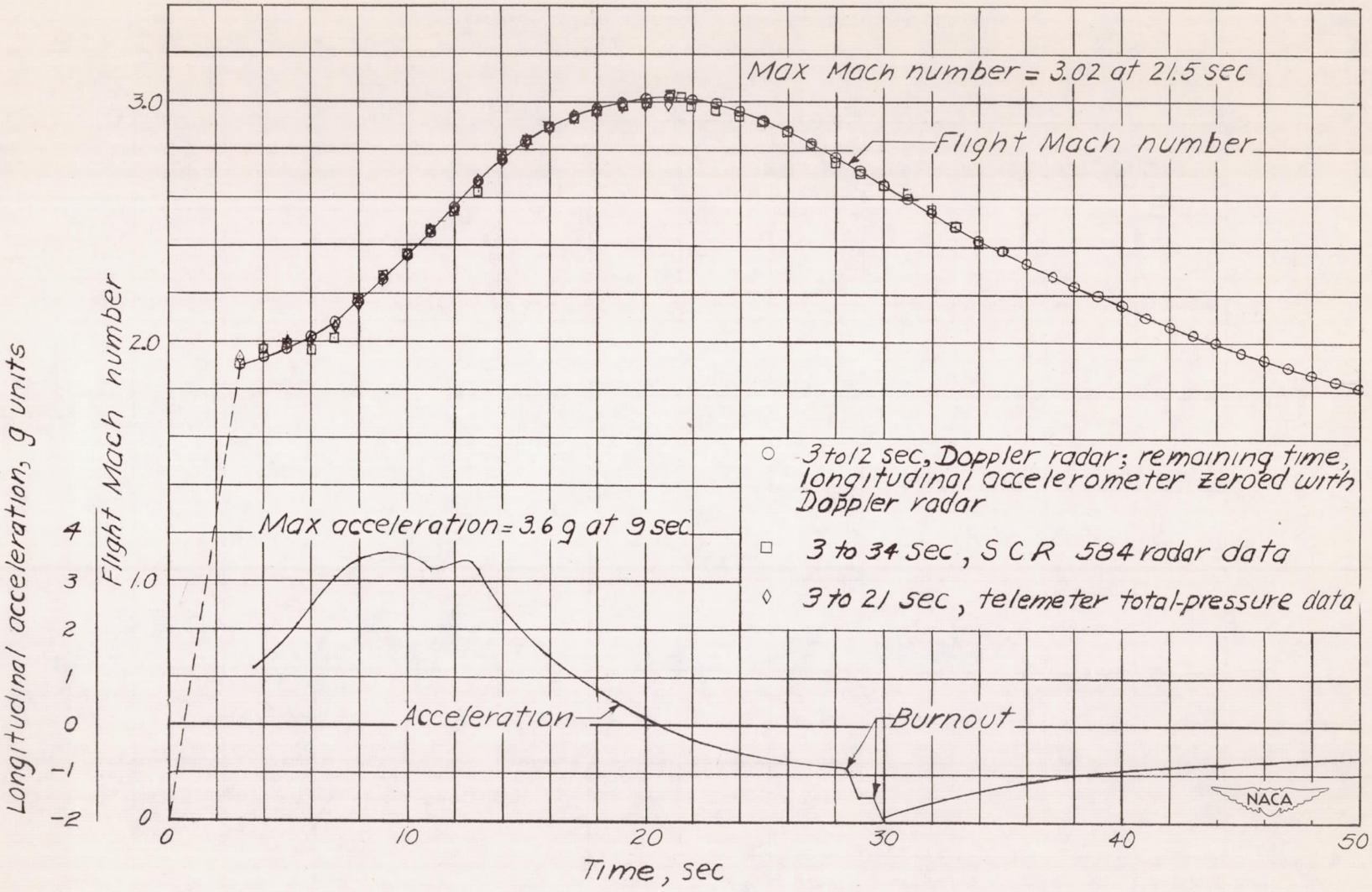

Figure 8.- Variation of flight Mach number with time.

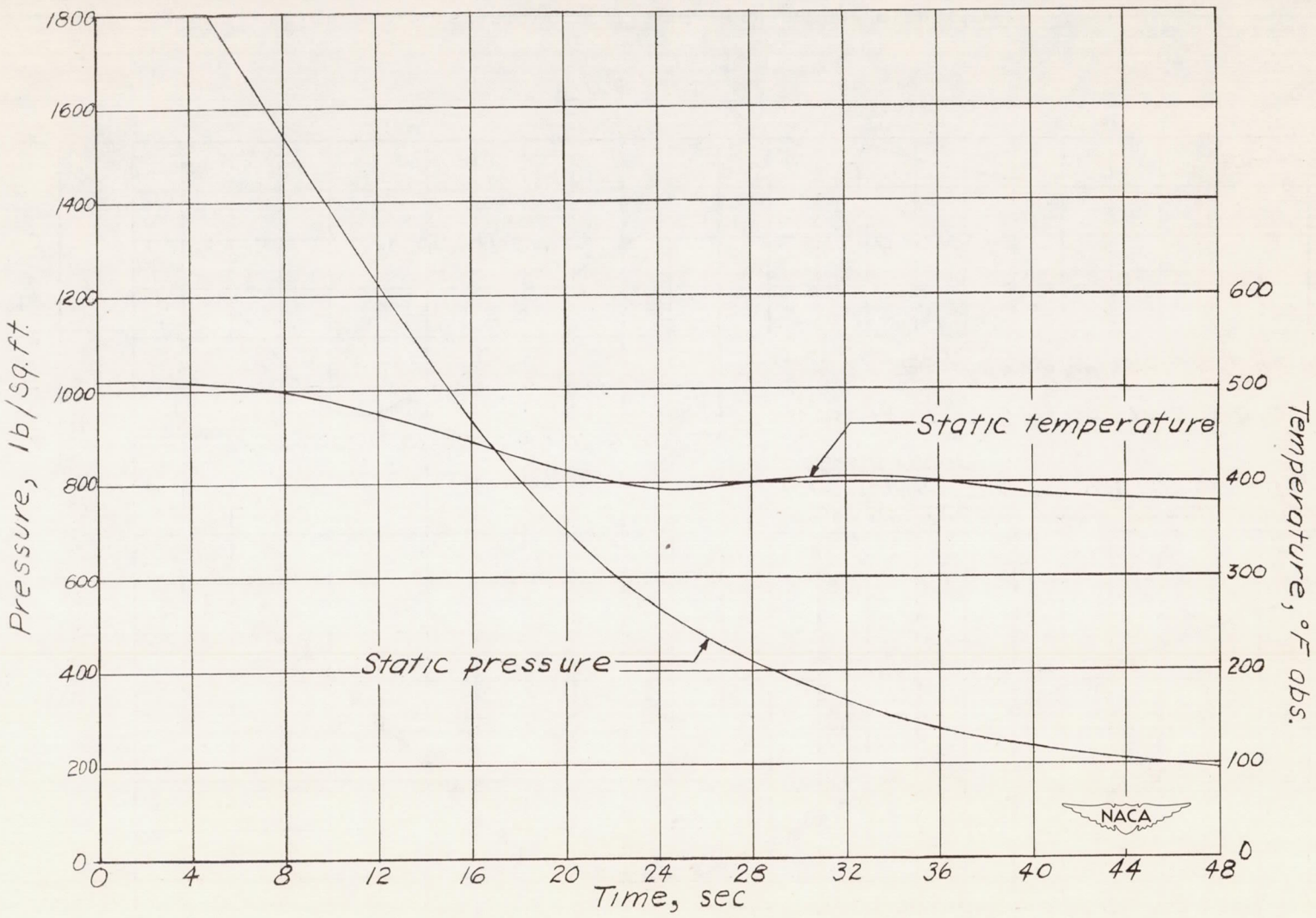

Figure 9.- Time history of atmospheric data.

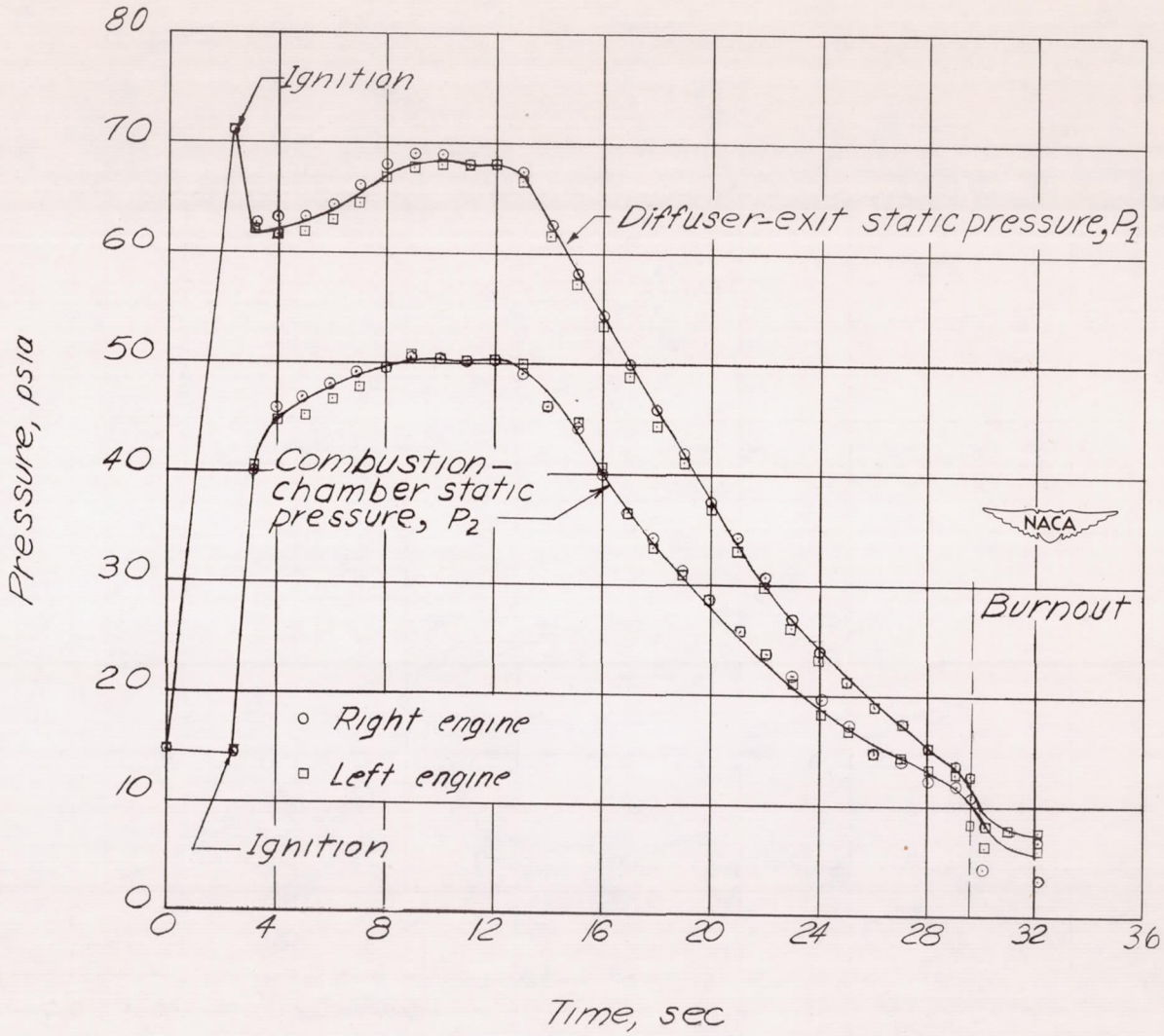

Figure 10.- Time history of engine static pressures.

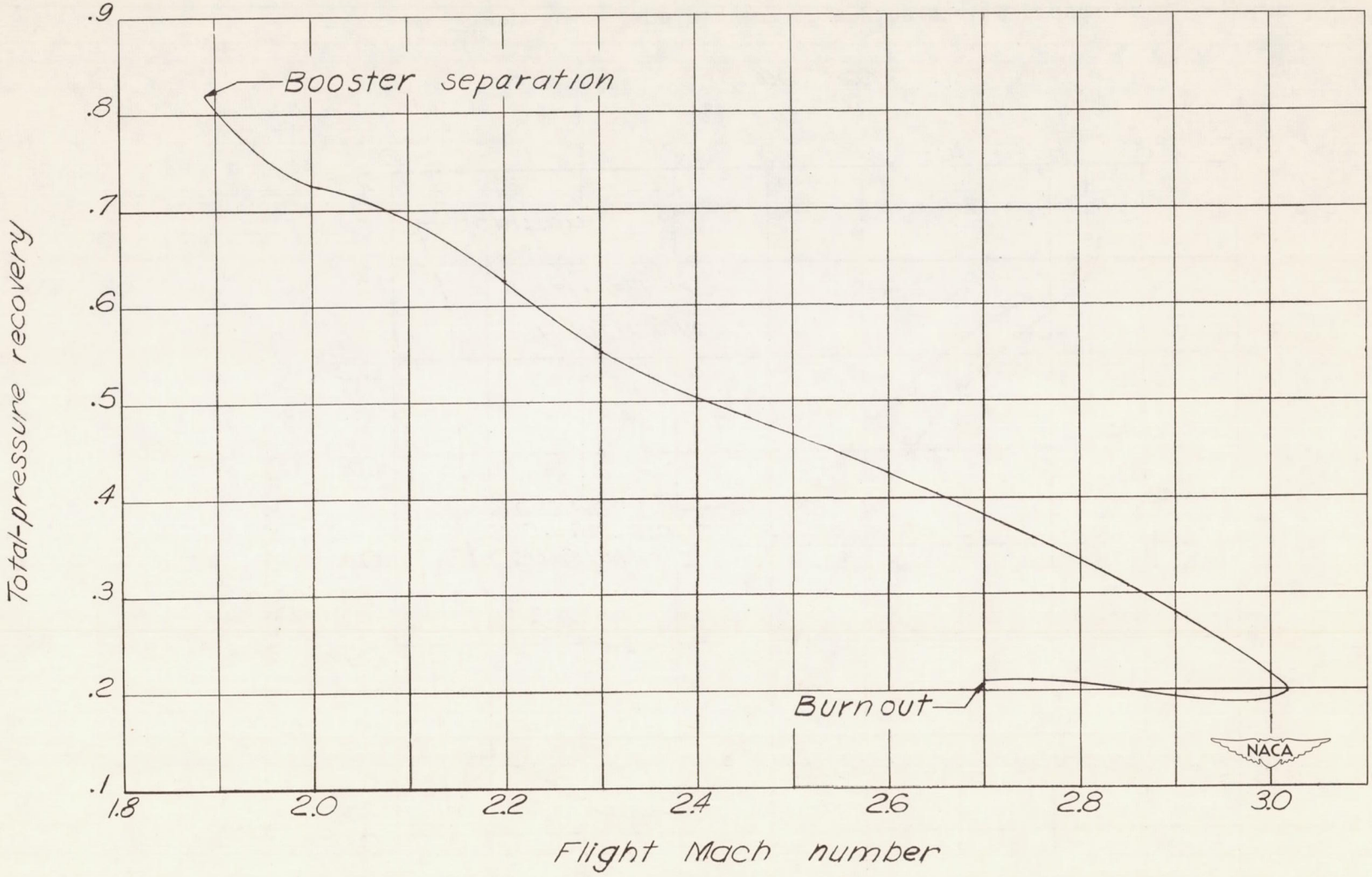

Figure 11.- Diffuser-total-pressure recovery as a function of Mach number.

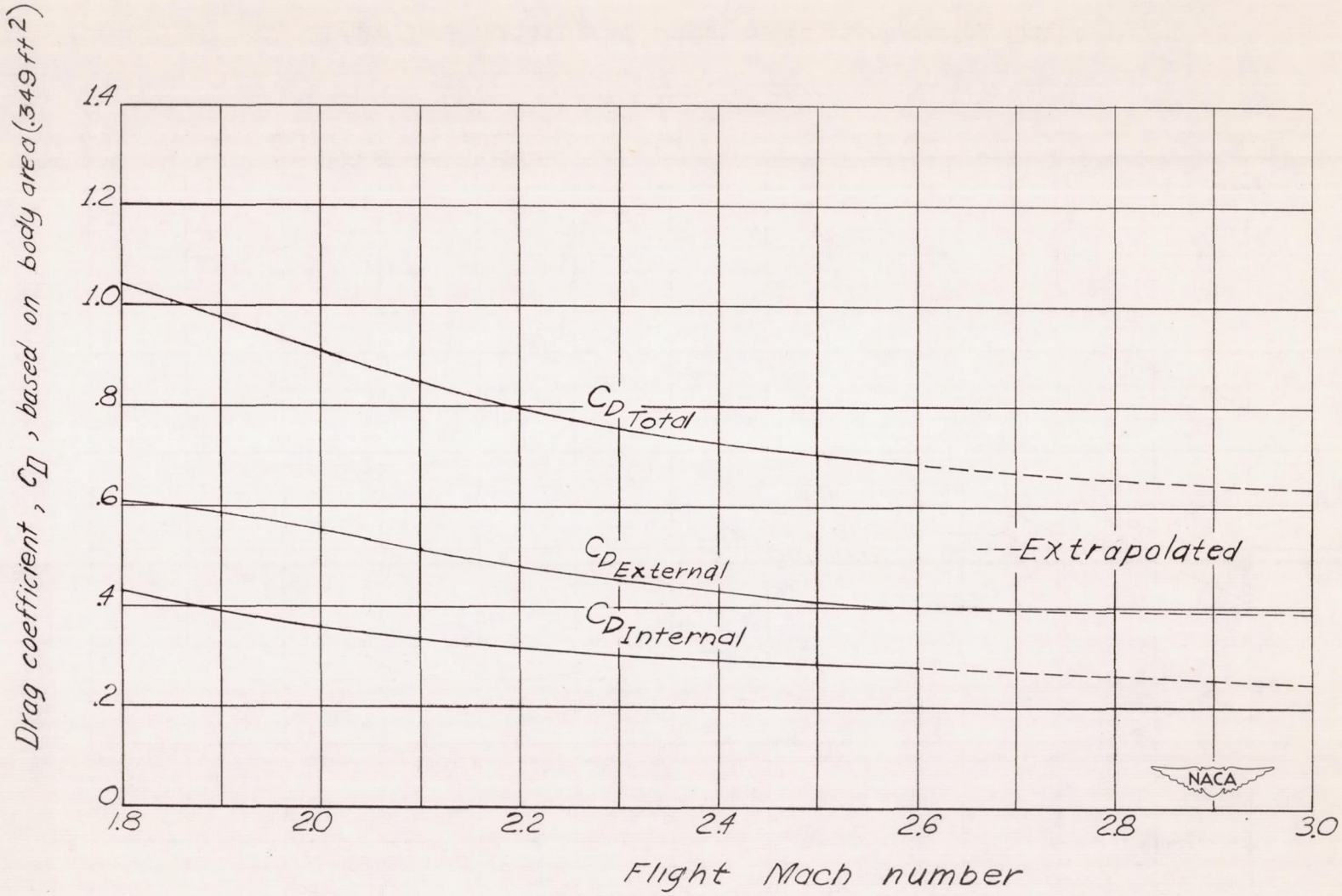

Figure 12.- Drag coefficient against Mach number for ram-jet test vehicle.

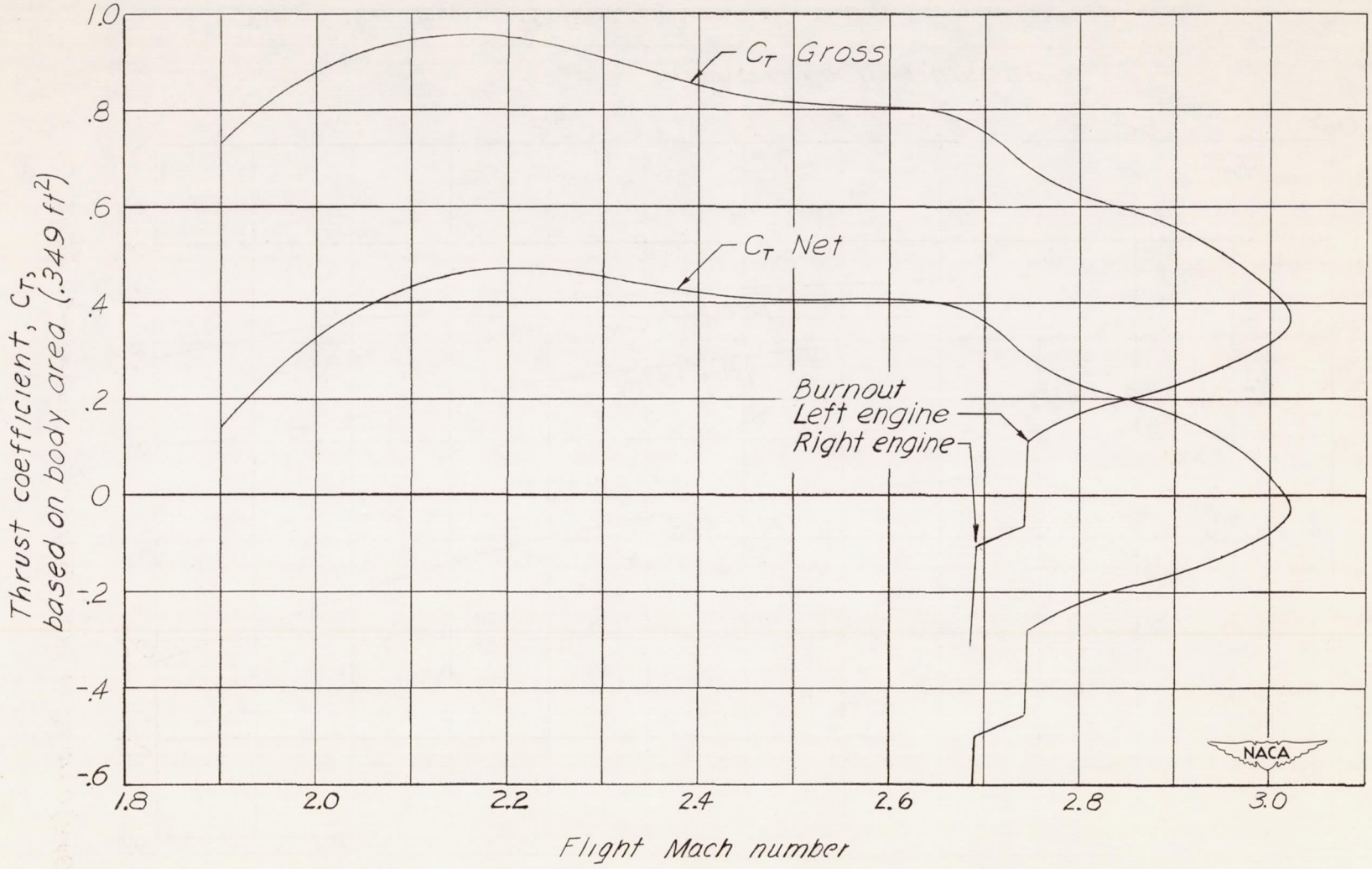

Figure 13.- Variation of thrust coefficient during flight.

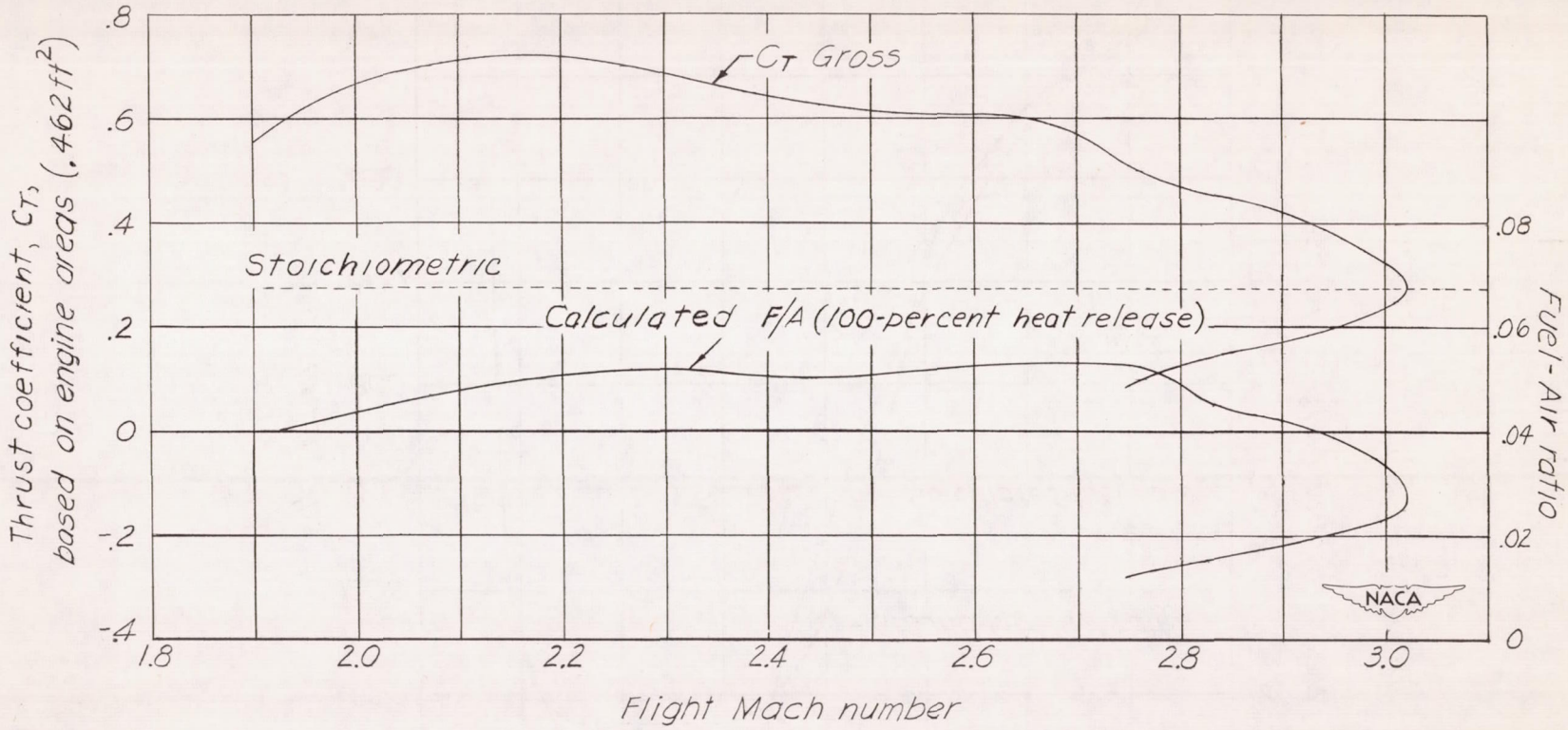

Figure 14.- Engine performance during flight.

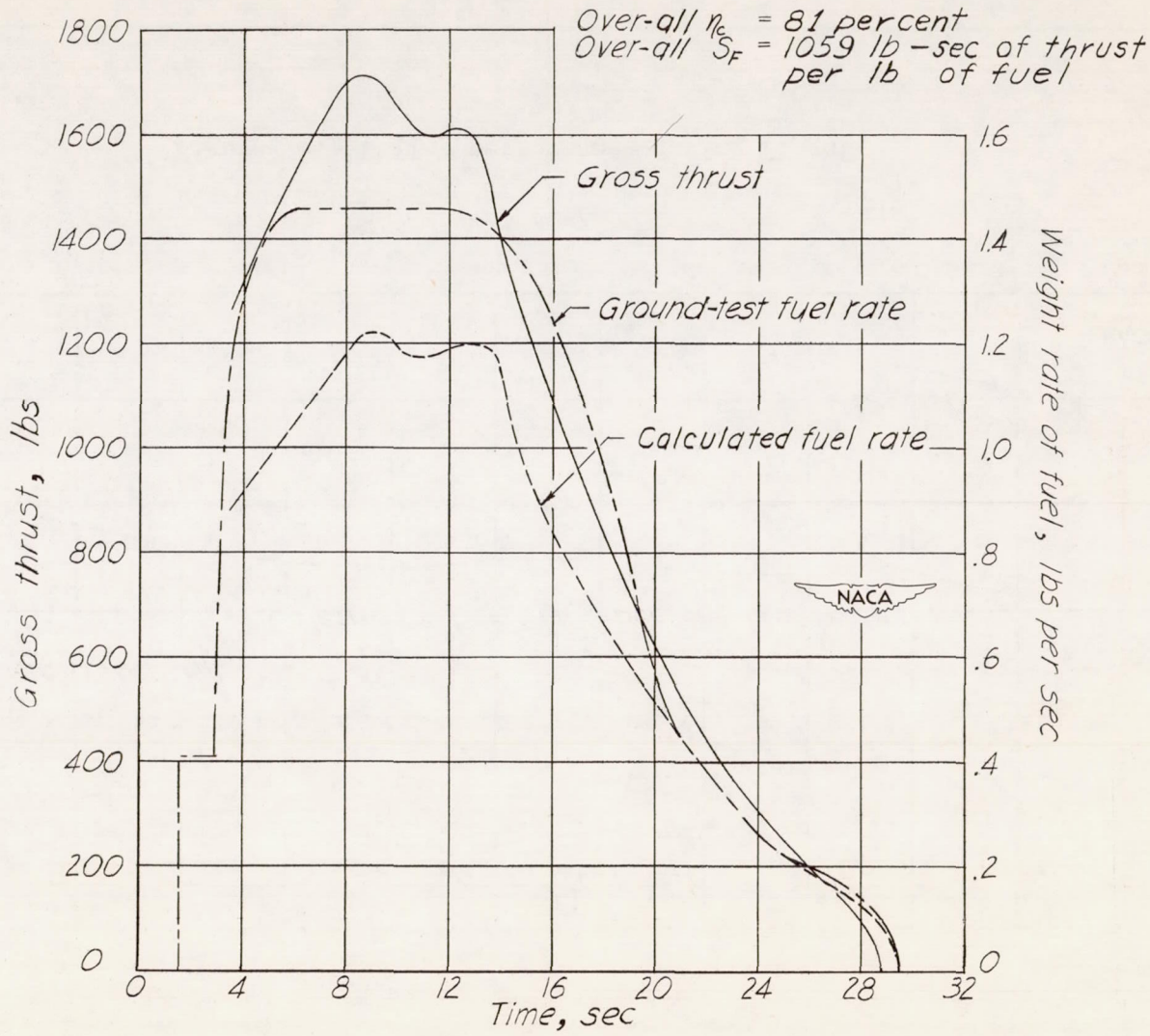

Figure 15.- Time history of total thrust and fuel consumption.